SHIP DETECTION IN SENTINEL-1 IMAGERY USING THE H-DOME TRANSFORMATION

[†‡]C.P. Schwegmann,[†‡]W. Kleynhans,[⋆‡]B.P. Salmon and [†‡]L. Mdakane

[†]Department of Electrical, Electronic and Computer Engineering, University of Pretoria, South Africa

[‡]Remote Sensing Research Unit, Meraka Institute, CSIR, Pretoria, South Africa
cschwegmann@csir.co.za

[⋆]School of Engineering, University of Tasmania, Australia

ABSTRACT

The ability to reliably detect ships within the ocean is one of the core capabilities of Maritime Domain Awareness. Constant improvements are pursued in both computational speed and reliable responses to events by exploring new ship detection methods. One such improvement is the availability of Sentinel-1 imagery. Owing to the fact that ships are considered locally bright objects, we propose using the H-dome transform to process the SAR image and improve ship detectability. The method was tested against two Sentinel-1 images in both HH and HV polarizations containing 82 ships. The method improved the false alarm rates when compared to the conventional cell-averaging Constant False Alarm Rate method at a minor reduction in detection accuracy.

***Index Terms*—** Marine technology, Synthetic aperture radar (SAR), Image Processing

1. INTRODUCTION

Improving the ability to detect ships within the ocean is an important goal for any country's Maritime Domain Awareness (MDA). Synthetic Aperture Radar (SAR) images acquired from space have historically been costly to obtain but the launch of the publicly available Sentinel-1 imagery has opened the research potential for many countries (seen in Fig. 1). SAR imagery assists with detecting and identifying of large ships participating in illegal, unreported and unregulated fishing (IUU) occurring in a country's exclusive economic zone (EEZ) which results in significant financial loss for that country [1, 2, 3].

Ship detection algorithms usually process SAR imagery with little pre-processing to preserve image statistics [4, 5]. Some advancements towards using alternative representations of the input image have been made in the form of wavelet processing [6]. In this paper we propose using the H-dome transform as a ship prescreening method on the new Sentinel-1 SAR images. The H-dome transform is a grayscale morphological operation which helps to highlight locally bright objects [7, 8].

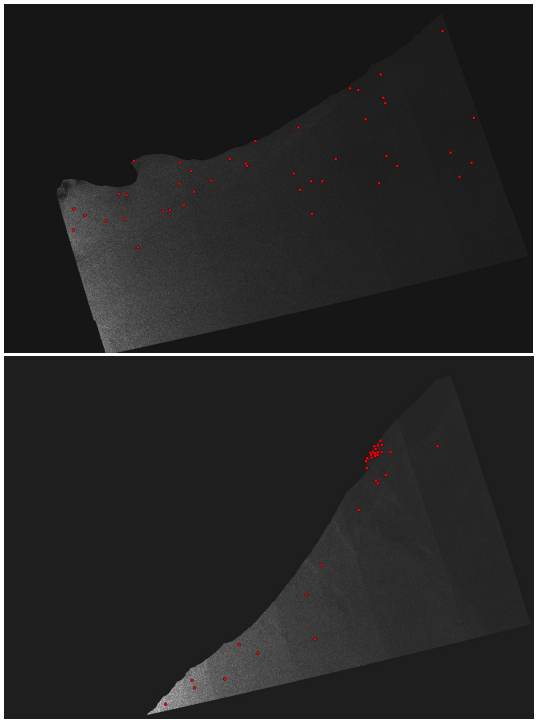

Fig. 1. Overview of the two Sentinel-1 EW SAR HH-polarized images, taken on the 6 and 8 October 2014 respectively. All land was removed from the input and the ships identified within the image are shown as red dots.

The paper is organized as follows: In section 2 we discuss the data used in our experiments followed by the detailed discussion of the proposed ship prescreening method in section 3. Sections 4 and 5 provides results and a concluding discussion about the method presented here.

2. DATA DESCRIPTION

Two Extra Wide Swath Mode (EW) Sentinel-1 Synthetic Aperture Radar (SAR) images were used in this study. Each

image has a spatial resolution of $20\,\text{m} \times 40\,\text{m}$ with a swath width of $400\,\text{km}$ in two polarizations namely HH and HV. The images were taken on 2014/10/06 and 2014/10/08 respectively. The images were acquired on the South African coast covering the cities of Port Elizabeth and Durban with a total of 82 ships. Two HH polarization images with all the land removed are shown in Fig. 1.

3. METHODOLOGY

The method proposed in this paper performs ship detection using a series of steps: Once the uncalibrated SAR image is geocoded and land masked, the H-dome transform is applied to the image. The result is then processed to detect cluster centroids which indicate the ships' positions. The following sections detail this procedure.

3.1. H-dome transform

The H-dome transform is a method for finding local maxima, often used in the medical field for finding sub-cellular structures [7, 8, 9]. The process identifies locally bright structures by cutting off their pixel values at a required minimum height h. All objects less than h are removed in the result H-dome transform image.

The method identifies locally bright objects using morphological grayscale reconstruction. To perform morphological grayscale reconstruction two images are required: a seed or marker image and a mask image. The mask image acts as a limit for which the seed image values are filled into. For this study the seed image is created by filtering the SAR image using a Laplacian of Gaussian filter [8]. The mask image is created by subtracting the chosen h value from the seed image. These two images are then processed using grayscale morphological reconstruction which produces a background or clutter image. This clutter image is subtracted from the original SAR image to produce the resulting H-dome transform image. This H-dome image highlights "domes" of local maxima which are at least of brightness h. The follow sections provide more details about these steps.

3.1.1. Laplacian of Guassian (LoG) filter

The Laplacian of Gaussian or Laplacian filter used in image processing for the detection of edges [10, 11]. The LoG operator highlights areas of rapidly varying intensity changes and highlights the edges of ships in SAR imagery with the kernel

$$LoG\left(x,y\right) = -\frac{1}{\pi\sigma_L^4}\left[1-\frac{x^2+y^2}{2\sigma_L^2}\right]\cdot\exp\left(-\frac{x^2+y^2}{2\sigma_L^2}\right). \tag{1}$$

The parameter σ_L is known as the scale parameter and is linked to the size of the objects being detected. The method is relatively robust against the choice in value as long as it is not unreasonably small (much less than 1.0) due to the large size of the ships compared to a single pixel (ships are in the order of 10 to 15 pixels in Sentinel-1 imagery). For the sake of this study it $\sigma_L = 1.0$. When this kernel is applied to the input image $I\left(x,y\right)$ it produces a resulting image $J\left(x,y\right)$. The height value h where $h > 0$ is subtracted from the $J\left(x,y\right)$ to produce the mask image $\hat{F}$ such that

$$\hat{F} = J\left(x,y\right) - h. \tag{2}$$

This mask image is then used in grayscale morphological reconstruction [7, 8], discussed next.

3.1.2. Grayscale morphological reconstruction

The next step of the method involves grayscale reconstruction of the seed image using the mask image generated by the LoG filter. Assume two input images $M\left(x,y\right)$ and $N\left(x,y\right)$ within the same discrete domain D [12]. If image $M\left(x,y\right)$ is called the seed or marker image and $N\left(x,y\right)$ is the mask image then the reconstruction of mask $N\left(x,y\right)$ from seed $M\left(x,y\right)$ is the union of connect components within $N\left(x,y\right)$ which contain at least a pixel of $M\left(x,y\right)$, for binary or grayscale images [12].

The input image $I\left(x,y\right)$ can be decomposed into two components: background structures (clutter) $B\left(x,y\right)$ and locally bright objects (ships) or H-dome component image $H\left(x,y\right)$. In this paper we construct $B\left(x,y\right)$ from the grayscale reconstruction mask image $\hat{F}$ and seed image $J\left(x,y\right)$ (the seed) [7, 8]. The locally bright objects can be extracted from the input image using the following

$$I\left(x,y\right) = H\left(x,y\right) + B\left(x,y\right), \tag{3}$$

$$H\left(x,y\right) = I\left(x,y\right) - B\left(x,y\right). \tag{4}$$

$H\left(x,y\right)$ is known as the H-dome transform of input image $I\left(x,y\right)$ and represents the areas of the image where local maxima or bright spots have at least an intensity value of h. The images $I\left(x,y\right)$, $J\left(x,y\right)$, $B\left(x,y\right)$ and $H\left(x,y\right)$ of a subimage from a Sentinel-1 image are shown in Fig. 2.

3.1.3. Ship discrimination

The H-dome transform provides another layer of the input image indicating the likelihood of a specific pixel being a bright object. Typically, the following stage of the H-dome detector uses a mean-shift clustering to find objects and their centers within $H\left(x,y\right)$ [7]. Mean Shift Clustering is a non-parametric estimation technique used to analyze images and other multi-modal data spaces [13]. The algorithm does not require a fixed number of clusters be known *a priori* and the shape of the clusters can be arbitrary. This works well for SAR imagery and the associated H-dome transformation $H\left(x,y\right)$ because the exact shape and number of ships is not known before processing the image. The single parameter of the mean-shift clustering algorithm is d which is the bandwidth or window radius and is used to determine how far apart

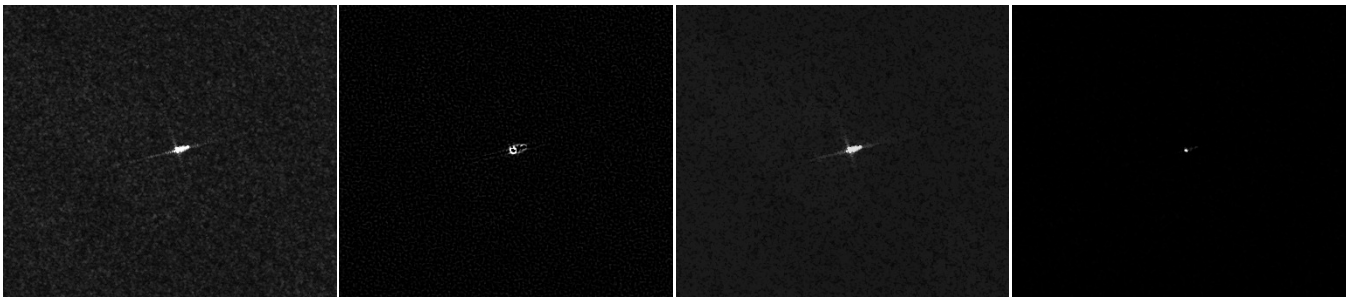

(a) (b) (c) (d)

Fig. 2. Four sub-images centered on a ship within the first Sentinel 1 image's HH polarization. The first sub-image (a) shows what the ship looks like before processing. Sub-image (b) shows the results of the LoG operator on the input sub-image. Sub-image (c) shows the image $B(x, y)$. Sub-image (d) shows the H-dome transform result from equation 4. Notice that the ship's contrast against the sea clutter is improved and the brightest part of the ship is clearly visible.

points are allowed to be to be grouped together. The detected centers of the clusters are used as the centers of the ships for detection purposes.

3.2. Clutter flattening

Looking closely at Fig. 2 (c) it can be seen that the clutter variation is much smaller than compared to the input SAR sub-image. Due to the fact that $B(x, y)$ can be processed as a separate image altogether, it can provide additional information about the clutter. Due to the process of the the H-dome transform the locally bright objects in $B(x, y)$ are flat as well and are cut off by the value h. This is exploited in [8] to create a rapid detector but in the case of a SAR ship detection it could be used as a threshold manifold within a method such as [14].

3.3. Ship structure highlighting

Looking at Fig. 2 (a) and comparing it to Fig. 2 (d) we notice that the brightest section of the ship can be seen much more clearly in (d). This is due to the property of the H-dome transform to highlight structures not typically visible (such as sub-cellular structures in [8]). This is a by-product of searching for the brightest local areas in the SAR image but it can be used as auxiliary information for subsequent steps in the processing of SAR images. Examples include orientation calculations or as ship type modeling (certain ships will have higher structures on the back/front thus having higher backscatter returns in that area).

4. RESULTS

The proposed ship detection method was compared using two metrics, Detection Accuracy and False Alarm Rate (FAR). Detection Accuracy is a measure of the number of correct detections or true positives obtained by the method whereas FAR is the number of false alarms divided by the total number of pixels tested for that image. The proposed method was tested against a cell-averaging constant false alarm rate (CA-CFAR) prescreening method to determine if the method is a viable ship prescreening method [1, 4, 5, 14]. This method is a widely used ship detection method that makes use of a window configuration to determine if each pixel is T times brighter than its neighbors. The proposed method is compared to the CA-CFAR prescreening method to determine if it is able to provide similar levels of performance to a baseline ship detector. The performance for the CA-CFAR method and the proposed method for the data in this study is shown in Table 1.

The CA-CFAR used in the comparison had a region of interest window size of 1×1, a guard window size of 11×11, background window size of 21×21 and threshold value of $T = 3.5$. The H-dome method used a $\sigma_L = 1.0$, $h = 230$ and $d = 5$. The results are presented first with the Detection Accuracy followed by the False Alarm Rate (FAR) in parenthesis.

The results indicates that both methods attained their respective lowest FAR within the first image in HH-polarization. Similarly, both methods obtained their best FAR within the second image's HV polarization. Across the four images, despite the fact that the H-dome transform method had lower detection accuracies it had better false alarm rates. Depending on the application, better false alarm rates may be more crucial and thus the loss in detection accuracy was deemed acceptable when compared to the improved FAR.

5. CONCLUSION

In this paper a novel method for ship detection using the H-dome transform was described. The method uses the notion that each image consists of a number of ship objects which can be segmented from the image by making use of local in-

Table 1. Detection Accuracy and False Alarm Rate (in parenthesis) for the two images with the conventional CA-CFAR and H-dome transformation methods.

Method	Image 1 (HH)	Image 1 (HV)	Image 2 (HH)	Image 2 (HV)
CA-CFAR	$97.61\%\ (1.85 \times 10^{-5})$	$95.91\%\ (8.93 \times 10^{-6})$	$96.96\%\ (1.98 \times 10^{-6})$	$100.0\%\ (1.33 \times 10^{-6})$
H-dome	$85.71\%\ (5.69 \times 10^{-5})$	$79.59\%\ (3.43 \times 10^{-7})$	$78.79\%\ (3.82 \times 10^{-7})$	$90.91\%\ (3.94 \times 10^{-7})$

tensity variation highlighting and morphological processing. The transformation greatly enhances the visibility of ships against the sea clutter but also affords a number of benefits including clutter flattening and sub-structure highlighting. Initial results indicate an improvement of FAR with an acceptable drop in detection accuracy. Future work includes combining other methods with the additional information generated by the H-dome features to improve ship detection performance within Sentinel-1 imagery.

6. REFERENCES

[1] C. P. Schwegmann, W. Kleynhans, and B. P. Salmon, "Ship Detection in South African oceans using SAR, CFAR and a Haar-like Feature Classifier," in *Geoscience and Remote Sensing Symposium, 2014. IGARSS 2014. IEEE International*, 2014, pp. 557–560.

[2] C. P. Schwegmann, W. Kleynhans, and B. P. Salmon, "Simulated Annealing CFAR Threshold Selection for South African Ship Detection in ASAR imagery," in *Geoscience and Remote Sensing Symposium, 2014. IGARSS 2014. IEEE International*, 2014, pp. 561–564.

[3] W. Kleynhans, B. P. Salmon, C. P. Schwegmann, and V. Seotlo, "Ship Detection in South African oceans using a combination of SAR and historic LRIT data," in *Geoscience and Remote Sensing Symposium, 2013. IGARSS 2013. IEEE International*, 2013, pp. 1–4.

[4] D. J. Crisp, "The State-of-the-Art in Ship Detection in Synthetic Aperture Radar Imagery," Tech. Rep. DSTO-RR-0272, DSTO Information Sciences Laboratory, Edinburgh, South Australia, May 2004.

[5] K. El-Darymli, P. McGuire, D. Power, and C. Moloney, "Target detection in synthetic aperture radar imagery: a state-of-the-art survey," *Journal of Applied Remote Sensinge*, vol. 7, no. 1, pp. 071598–071598, Mar. 2O13.

[6] F. Berizzi D. Stagliano, A. Lupidi, "Ship detection from sar images based on CFAR and wavelet transform," in *2012 Tyrrhenian Workshop on Advances in Radar and Remote Sensing (TyWRRS)*, Sept. 2012, pp. 53–58.

[7] P. Ruusuvuori et al., "Evaluation of methods for detection of fluorescence labeled subcellular objects in microscope images,," *BMC Bioinformatics*, vol. 11, no. 1, pp. 1471–2105, Apr. 2010.

[8] W. Niessen E. Meijering I. Smal, M. Loog, "Quantitative Comparison of Spot Detection Methods in Fluorescence Microscopy,," *IEEE Transactions on Medical Imaging*, vol. 29, no. 2, pp. 282–301, Feb. 2010.

[9] D. Bloomberg, "Grayscale Morphology," http://www.leptonica.com/grayscale-morphology.html, 2015, Accessed: 2015-01-05.

[10] A. Walker E. Wolfart R. Fisher, S. Perkins, "Laplacian/Laplacian of Gaussian," http://homepages.inf.ed.ac.uk/rbf/HIPR2/log.htm, 2003, Accessed: 2015-02-25.

[11] D. Marr, *Vision*, W. H. Freeman, San Fransisco, California, 1982.

[12] L. Vincent, "Morphological grayscale reconstruction: definition, efficient algorithm and applications in image analysis," in *1992 IEEE Computer Vision and Pattern Recognition (CVPR)*, 1993, pp. 633–635.

[13] D. Comanicius and P. Meer, "Mean Shift: A Robust Approach Toward Feature Space Analysis," *IEEE Transactions On Pattern Analysis and Machine Intelligence*, vol. 24, no. 5, pp. 1–18, May 2002.

[14] C. Schwegmann, W. Kleynhans, and B. Salmon, "Manifold Adaptation for Constant False Alarm Rate Ship Detection in South African Oceans," *IEEE Journal of Selected Topics in Applied Earth Observations and Remote Sensing*, vol. PP, no. 99, pp. 1–9, Apr. 2015.